Gene Expression Changes Associated with Myocarditis and Fibrosis in Hearts of Mice with Chronic Chagasic Cardiomyopathy

Milena Botelho Pereira Soares,[1,2] Ricardo Santana de Lima,[1] Leonardo Lima Rocha,[1] Juliana Fraga Vasconcelos,[1] Silvia Regina Rogatto,[3,4] Ricardo Ribeiro dos Santos,[1,2] Sanda Iacobas,[7] Regina Coeli Goldenberg,[5] Dumitru Andrei Iacobas,[7] Herbert Bernard Tanowitz,[8,9] Antonio Carlos Campos de Carvalho,[5,6] and David Conover Spray[7,8]

[1]Centro de Pesquisas Gonçalo Moniz, Fundação Oswaldo Cruz, and [2]Hospital São Rafael, Salvador, [3]Departamento de Urologia, Faculdade de Medicina, Universidade do Estado de São Paulo, Botucatu, [4]Hospital do Câncer A. C. Camargo, São Paulo, and [5]Instituto de Biofísica Carlos Chagas Filho, Universidade Federal do Rio de Janeiro, and [6]Instituto Nacional de Cardiologia, Rio de Janeiro, Brazil; [7]D. P. Purpura Department of Neuroscience, [8]Department of Medicine, and [9]Department of Pathology, Albert Einstein College of Medicine, Bronx, New York

Chronic chagasic cardiomyopathy is a leading cause of heart failure in Latin American countries. About 30% of *Trypanosoma cruzi*–infected individuals develop this severe symptomatic form of the disease, characterized by intense inflammatory response accompanied by fibrosis in the heart. We performed an extensive microarray analysis of hearts from a mouse model of this disease and identified significant alterations in expression of ~12% of the sampled genes. Extensive up-regulations were associated with immune-inflammatory responses (chemokines, adhesion molecules, cathepsins, and major histocompatibility complex molecules) and fibrosis (extracellular matrix components, lysyl oxidase, and tissue inhibitor of metalloproteinase 1). Our results indicate potentially relevant factors involved in the pathogenesis of the disease that may provide new therapeutic targets in chronic Chagas disease.

Chagas disease, caused by infection with the protozoan *Trypanosoma cruzi*, is still a major health problem in Latin America, where it affects 16–18 million people [1]. The most common chronic form, chagasic cardiomyopathy (CCM), is a fatal disease for which there is no effective treatment available other than heart transplantation. CCM is characterized by focal or disseminated inflammation causing myocytolysis, necrosis, and progressive fibrosis [2–4].

The pathological basis of CCM is multifactorial [5, 6]. It may in part result from inflammatory responses to *T. cruzi* antigen, to cardiac autoantigens, or to both types of antigens [7]. A prominent role of parasite antigens in this pathology has been supported by the demonstration that a decrease in parasite load caused a reduction in myocarditis and cardiac disturbances in mice chronically infected with *T. cruzi* [8].

The identification of factors involved in the establishment of chronic heart lesions is of great interest for the development of new therapeutic strategies for patients with this fatal disease. In this study we performed a DNA microarray analysis to identify alterations in gene expression in the myocardium of mice chronically infected with the Colombian strain of *T. cruzi*, compared with uninfected counterparts. Our results indicate a profound effect on expression of a number of genes related to inflammation and fibrosis in the hearts of mice with CCM.

METHODS

Trypomastigotes of Colombian *T. cruzi* strain [9] were obtained from culture supernatants of infected LCC-MK2 cells. C57Bl/6 male and female mice were infected by intraperitoneal injection of *T. cruzi* trypomastigotes. Parasitemia was evaluated at various times after infection by counting the number of trypomastigotes in peripheral blood aliquots. Animals were raised and maintained at the Gonçalo Moniz Research Center/Fundação Oswaldo Cruz (FIOCRUZ) and provided with rodent diet and water ad libitum. Animals were handled according to the National Institutes of Health guidelines for animal experimentation. All procedures described here had prior approval from the local animal ethics committee.

Mice were killed after 8 months of infection, and their hearts removed and fixed in 10% buffered formalin. Morphometric analyses were performed in hematoxylin-eosin– or Sirius red–stained heart sections captured using a digital camera adapted to a BX41 microscope (Olympus). Images were analyzed using Image-Pro Program software (version 5.0; Media Cybernetics).

Frozen heart sections were used for detection of CD4, CD8, CD11b, intercellular adhesion molecule 1 (ICAM-1), and major histocompatibility complex (MHC) class II expression by immunofluorescence, using specific antibodies (BD Biosciences) followed by streptavidin (Alexa Fluor 568; Molecular Probes). The myocardium was stained with phalloidin (Molecular Probes) or an anti–cardiac myosin antibody (Sigma). Nuclei were stained with 4,6-diamidino-2-phenylindole (DAPI) (Vectashield HardSet mounting medium with DAPI H-1500; Vector Laboratories). Sections were analyzed using a BX61 microscope equipped with epifluorescence and appropriate filters (Olympus) and a system to enhance the fluorescence resolution (OptiGrid; Thales Optem).

Stromal cell–derived factor 1 (SDF-1), tumor necrosis factor (TNF) α, and interferon (IFN) γ concentrations were measured in total heart extracts. Heart proteins were extracted from 100 mg tissue/mL phosphate-buffered saline, to which 0.4 mol/L sodium chloride, 0.05% Tween 20, and protease inhibitors (0.1 mmol/L phenylmethylsulfonyl fluoride, 0.1 mmol/L benzethonium chloride, 10 mmol/L ethylenediaminetetraacetic acid, and 20-KI aprotinin A/100 mL) were added. The samples were centrifuged for 10 min at 3000 *g*, and the supernatant was kept frozen at −70°C. Cytokine levels were estimated using commercially available enzyme-linked immunosorbent assay kits for mouse SDF-1, TNF-α, and IFN-γ (R&D Systems), according to the manufacturer's instructions. Reaction was revealed after incubation with streptavidin–horseradish peroxidase conjugate, followed by detection using 3,3′,5,5′-tetramethylbenzidine peroxidase substrate and reading at 450 nm.

Hearts of normal and *T. cruzi*–infected mice were extracted and quickly frozen in liquid nitrogen for 5 min. The material was ground, and RNA extraction was performed using RNeasy Mini Kit (Qiagen), following the manufacturer's instructions. After addition of 1 U/μL DNase I (Invitrogen), the complementary DNA (cDNA) was obtained using SuperScript II Reverse Transcriptase (Invitrogen) in a final volume of 30 μL. Reaction cycles were performed on an Eppendorf Mastercycler gradient for 1 h (42°C for 60 min; 70°C for 15 min). Polymerase chain reaction (PCR) amplification was performed in an ABI Prism 7000 Sequence Detection System (Applied Biosystems). Primers and TaqMan probe for *Timp1*, the glyceraldehyde 3-phosphate dehydrogenase control reference gene, were designed and synthesized according to Assay-by-Design (Applied Biosystems). Quantitative data were analyzed using Sequence Detection System software (version 1.0; Applied Biosystems). PCRs were carried out in a total volume of 25 mL, according to the manufacturer's instructions. The standard curves of the target and reference genes showed similar results for efficacy (>90%). The relative quantification was given by the ratio between the mean values of the target gene and the reference gene (*Gapdh*) in each sample. The relative amount of PCR product generated from each primer set was determined on the basis of the cycle threshold (Ct) value. The relative quantification was calculated by the $2^{-\Delta\Delta Ct}$ method (Ct, fluorescence threshold value; ΔCt, the Ct of the target gene minus the Ct of the reference gene; $\Delta\Delta$Ct, the infected sample ΔCt minus the reference sample ΔCt).

Total RNA (20 μg) extracted from each of the 4 control and 4 infected hearts was reverse transcribed into cDNA incorporating fluorescent Alexa Fluor_647 or Alexa Fluor_555–aha-dUTPs (Invitrogen), by means of the SuperScript Plus Direct cDNA Labeling System (Invitrogen). Differently labeled biological replicas were cohybridized overnight at 50°C with MO30N mouse oligonucleotide arrays spotted with 32,620 70mer Operon oligonucleotides (Duke Microarray Facility; version 3.0.1) (https://www.ncbi.nlm.nih.gov/geo/query/acc.cgi?acc=GPL8938) using the "multiple yellow" strategy described elsewhere [10]. In this strategy, differently labeled biological replicas are cohybridized with the array. Thus, we have hybridized 2 arrays with samples from 4 control hearts and 2 other arrays with samples from 4 infected hearts. After washing (0.1% sodium dodecyl sulfate and 1% saline-sodium citrate) to remove the nonhybridized cDNAs, each array was scanned with an Axon 4000B dual-laser scanner (MDS Analytical Technologies) and images were primarily analyzed with GenePix Pro software (version 6.0; Axon Instruments). Locally corrupted or saturated spots, as well as those for which the foreground median fluorescence did not exceed twice the median local background fluorescence in 1 sample, were eliminated from analysis in all samples.

Microarray data were processed as described in our other studies [10–12]. In brief, we used a normalization algorithm that alternates intrachip and interchip normalization of the net

fluorescence (ie, background-subtracted foreground) signals of the validated spots until the residual error is <5% in subsequent steps. Intrachip normalization balances the averages of net fluorescence values in the 2 channels within each pin domain (subset of spots printed by the same pin), corrects the intensity-dependent bias (usually referred as Lowess normalization), and forces the standard distribution (mean, 0; standard deviation, 1) of $\log_2$ ratios (scale normalization) for net fluorescent values in the 2 channels for each array. Interchip normalization assigns a ratio between the corrected net fluorescence of each valid spot and the average net fluorescence of all valid spots in both control (C1, C2, C3, and C4) and infected (I1, I2, I3, and I4) samples. The spots probing the same gene were organized into redundancy groups, and their background-subtracted fluorescence was replaced by a weighted average value. A gene was considered significantly up- or down-regulated in the comparison between 4 infected and 4 control hearts if the absolute fold change was >1.5 and the P value was <.05 (Student's heteroscedastic t test of equality of the mean distributions, with Bonferroni-type adjustment for redundancy groups). Gen-MAPP [13] and MAPPFinder software (http://www.genmapp .org) and databases were used to identify the most affected gene ontology categories.

Morphometric, quantitative reverse-transcription PCR, and cytokine data were analyzed using Student's t test. Differences were considered significant at $P < .05$.

RESULTS

CCM caused by chronic infection with Colombian strain T. cruzi in C57Bl/6 mice.
On infection with 1000 trypomastigote forms of Colombian strain *T. cruzi*, C57Bl/6 mice develop blood parasitemia peaking at ∼35 days after infection (Figure 1A). The mortality rate reached 28.5% during the first 100 days (Figure 1B) and ∼31.4% after 8 months of infection. Progressive myocarditis accompanied by fibrosis occurs after the acute phase of infection. At 8 months of infection, heart sections from chagasic mice revealed a multifocal inflammatory response composed mainly of mononuclear cells (Figure 1C and 1E) and exhibited areas of fibrosis (Figure 1D and 1F).

Global gene expression analysis.
Microarray data from this experiment have been deposited in GenBank (https://www .ncbi.nlm.nih.gov/geo/query/acc.cgi?acc=GSE17363). When control hearts from C57Bl/6 mice were compared with those from age- and sex-matched mice chronically infected with the Colombian strain of *T. cruzi*, genes differentially expressed were detected. Spots corresponding to 14,356 unigenes satisfied the criteria of adequate quantitation for all 8 RNA samples. Of these, 1221 (8.5%) were significantly up-regulated in the chagasic hearts and 494 (3.4%) were significantly down-regulated (>50% difference; $P < .05$). A list of all genes that were found to be differentially expressed is presented in Table 1, and subsets

of the genes showing higher fold change in expression ratio are considered below.

Pathways of proteins encoded by genes that were significantly affected by parasitic infection were determined using Gen-MAPP software (http://www.genmapp.org), in which significance is assessed by whether regulated genes are disproportionately represented within a gene ontology term. Pathways of genes significantly up-regulated in infected hearts ($P < .05$) are listed in Table 2 and prominently include immune response and related terms (eg, inflammatory response, intracellular signaling cascade, and chemokine and cytokine receptor activity). Results of the GenMAPP analysis of these altered genes are shown in Figure 2A. In addition, up-regulated pathways include phosphate transport, cell proliferation, and actin binding (eg, Arp2/3 protein complex and actin filament organization, cytoskeleton, and membrane ruffling). These genes related to the actin cytoskeleton are illustrated in Figure 2B. In addition to these well-represented pathways, smaller pathways showed prominent perturbation, including genes involved in cardiac differentiation (*Tgfb2* and *Itgb1*) and regulation of action potential (*Gnaq*, *Hexa*, *Hab1*, and *Cd9*).

Pathways containing an overrepresentation of down-regulated genes (Table 2) included mitochondrion, enzymatic activity of several types, and tyrosine kinase signaling. Genes down-regulated in less extensive pathways included negative regulation of notch plus bone morphometric protein signaling (*Htra1* and *Twsg1*) and regulation of vascular endothelial growth factor receptor signaling (*Flt1*).

Mice chronically infected with the Colombian strain of *T. cruzi* have intense myocarditis (Figure 1E). The inflammatory infiltrate is mainly composed by mononuclear cells, including CD4$^+$ and CD8$^+$ T lymphocytes (Figure 3A and 3B) and macrophages (Figure 3C). The analysis of genes that were up-regulated ≥5-fold in the arrays showed alterations in a number of genes related to inflammation and immune responses. Genes coding for the macrophage cell surface marker CD68 and the lymphocyte antigens CD38 and CD52 had their expression increased in chronic chagasic hearts (Table 3), a finding compatible with the presence of these cells in the inflammatory infiltrate.

Up-regulation of genes coding for chemoattractant factors Ccl2, Ccl7, Ccl8, and Ccl12 was observed (Table 3). Immunocytochemistry confirmed that the levels of Ccl12 (SDF-1) in hearts of chronically chagasic mice were increased in comparison with those of normal mice (Figure 4A). In addition, the expression of phospholipase A2, group VII (platelet-activating factor [PAF] acetylhydrolase), and complement factor B genes were highly increased (47.6- and 42.5-fold, respectively) by chronic infection (Table 3).

The expression of genes coding for adhesion molecules, such as galectin-3, P-selectin ligand (CD162), integrin $\beta3$ (CD61),
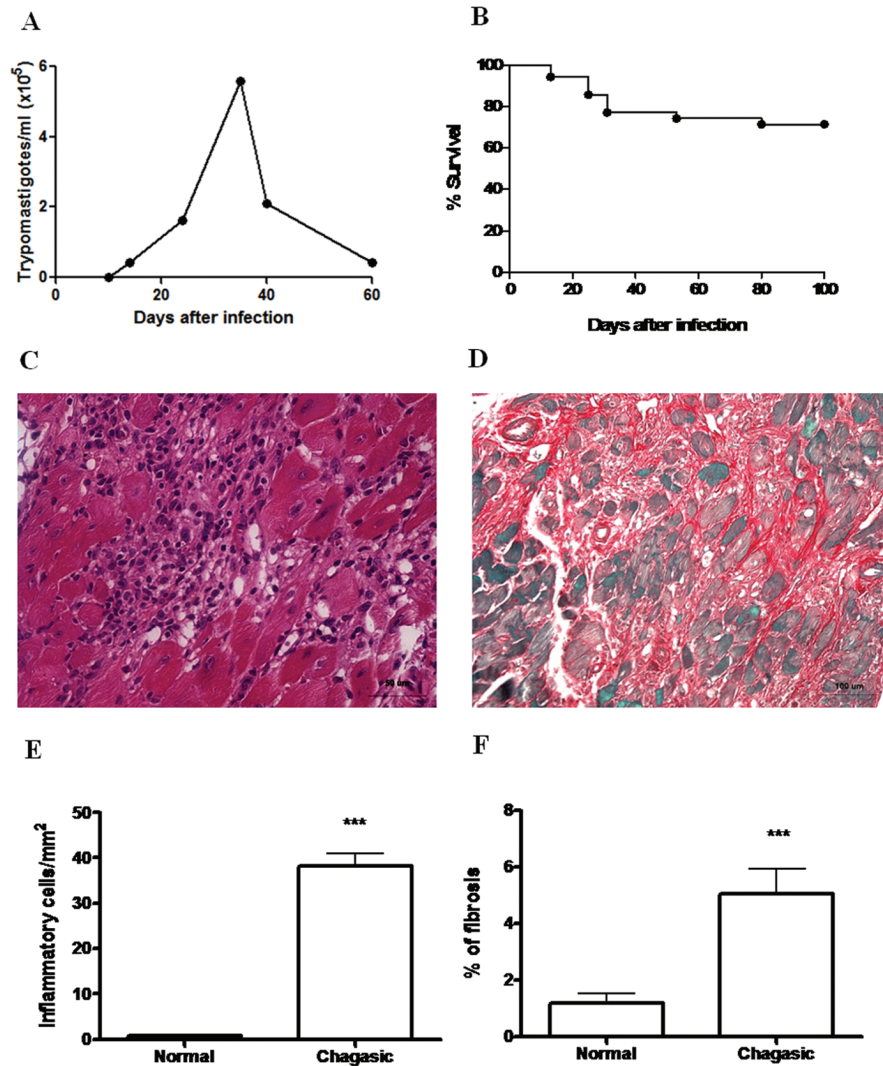
Figure 1. Infection of C57Bl/6 mice with Colombian strain *Trypanosoma cruzi*. Mice ($n = 35$) were infected with 1000 Colombian strain trypomastigotes. *A* and *B*, Parasitemia (*A*) and mortality (*B*) evaluated during the acute phase of infection. Data in panel A represent medians for individual parasitemia. *C* and *D*, Inflammation (*C*) and fibrosis (*D*) evidenced in heart sections from mice 8 months after infection, stained with hematoxylineosin and Sirius red. *E* and *F*, Morphometric quantification of inflammatory cells (*E*) and fibrosis area (*F*) in heart sections from normal mice ($n = 4$) and chagasic mice ($n = 9$; 8 months after infection with *T. cruzi*). Bars represent means $\pm$ standard errors of the mean. ***$P < .05$.

and ICAM-1 (CD54), was increased in hearts of chagasic mice (Table 3). Immunostaining revealed that ICAM-1 is virtually absent in control hearts, but in hearts of infected mice it is found mainly in inflammatory and endothelial cells (Figure 3*D* and 3*E*). The expression of genes coding for several cathepsins, proteases important in lysosomal degradation, was also upregulated (Table 3). Of special interest is cathepsin S, which mediates degradation of the invariant Ii chain in antigen-presenting cells [13]. The expression of genes coding for MHC class II molecules IEb and IAa were highly altered. MHC class II molecules were observed to be highly expressed in cells of the inflammatory infiltrate in infected hearts (Figure 3*F* and 3*G*). In addition, the expression of genes encoding 2 proteasome subunits was also up-regulated (Table 3).

Cytokine-associated genes were differentially expressed in hearts of chagasic mice (Table 3). Of special interest is upregulation of genes associated with 2 cytokines related to the severe form of chronic CCM [14, 15], IFN-γ (*Igtp*, *Ifi30*, *Ifi47*, *Irf1*, and *Irf5*) and TNF-α (*Tnfaip2*, *Tnfrsf1b*, and *Litaf*). Although regulation of genes encoding IFN-γ and TNF-α could not be analyzed in this microarray data set owing to technical problems, the protein levels of both cytokines were increased

Table 1.   Genes Found to Be Differentially Regulated

This table is available in its entirety in the online version of the *Journal of Infectious Diseases*

Table 2. Up-regulated and Down-regulated Gene Ontology (GO) Categories in *Trypanosoma cruzi*–Infected Hearts

GOID	GO name	Type	No. measured[a]	Change, %	Z score	Permuted P
Up-regulated						
1726	Ruffle	C	21	38.10	5.039	<.001
6955	Immune response	P	108	19.44	4.817	<.001
8009	Chemokine activity	F	19	36.84	4.592	<.001
5764	Lysosome	C	44	31.82	4.487	<.001
5783	Endoplasmic reticulum	C	305	14.43	3.806	<.001
7242	Intracellular signaling cascade	P	169	12.43	3.302	<.001
6935	Chemotaxis	P	31	25.81	3.254	.004
30036	Actin cytoskeleton organization and biogenesis	P	32	12.50	3.232	.002
4180	Carboxypeptidase activity	F	11	27.27	3.22	.007
16798	Hydrolase activity, acting on glycosyl bonds	F	25	28.00	3.172	.004
15629	Actin cytoskeleton	C	40	10.00	3.09	.007
5938	Cell cortex	C	10	20.00	3.035	.01
7015	Actin filament organization	P	15	26.67	2.914	.015
5279	Amino acid–polyamine transporter activity	F	11	18.18	2.91	.016
42552	Myelination	P	13	23.08	2.806	.024
8285	Negative regulation of cell proliferation	P	45	15.56	2.67	.015
8284	Positive regulation of cell proliferation	P	56	16.07	2.669	.014
45596	Negative regulation on cell differentiation	P	13	7.69	2.603	.014
8283	Cell proliferation	P	55	16.36	2.588	.012
8201	Heparin binding	F	28	21.43	2.585	.019
6954	Inflammatory response	P	67	11.94	2.582	.008
9986	Cell surface	C	43	18.60	2.347	.026
6817	Phosphate transport	P	40	17.50	2.18	.039
4896	Hematopoietin/interferon class (D200 domain) cytokine receptor activity	F	16	25.00	2.18	.048
48754	Branching morphogenesis of a tube	P	12	33.33	2.123	.048
45165	Cell fate commitment	P	16	12.50	2.113	.038
42127	Regulation of cell proliferation	P	17	0.00	2.055	.045
7264	Small GTPase-mediated signal transduction	P	83	10.84	2.055	.05
Down-regulated						
5739	Mitochondrion	C	351	17.38	13.839	<.001
5737	Cytoplasm	C	613	2.61	5.628	<.001
3824	Catalytic activity	F	104	5.77	5.241	<.001
16491	Oxidoreductase activity	F	208	6.73	4.835	<.001
3954	NADH dehydrogenase activity	F	10	30.00	4.599	.005
50660	FAD binding	F	34	17.65	4.541	<.001
30170	Pyridoxal phosphate binding	F	31	16.13	3.871	.002
5777	Peroxisome	C	51	13.73	3.839	.002
6118	Electron transport	P	189	7.41	3.727	<.001
9055	Electron carrier activity	F	60	8.33	3.349	.003
5975	Carbohydrate metabolic process	P	81	6.17	3.169	.001
16874	Ligase activity	F	121	8.26	3.123	.005
8483	Transaminase activity	F	10	20.00	2.947	.017
7169	Transmembrane receptor protein tyrosine kinase signaling pathway	P	30	13.33	2.801	.012
6631	Fatty acid metabolic process	P	33	12.12	2.735	.013
166	Nucleotide binding	F	715	3.78	2.698	.007
9058	Biosynthetic process	P	31	12.90	2.511	.009
7050	Cell cycle arrest	P	24	12.50	2.43	.034
8152	Metabolic process	P	288	8.68	2.319	.025
6629	Lipid metabolic process	P	87	8.05	2.041	.043
16740	Transferase activity	F	558	4.84	1.995	.044

NOTE. C, cellular location; F, molecular function; FAD, flavin adenine dinucleotide; GOID, GO identification no.; NADH, nicotinamide adenine dinucleotide, reduced; P, biological process.

[a] No. of genes analyzed in that GOID.

Figure 2. Genes found to be altered within the category of immune response and related terms from the GenMAPP database (Gladstone Institute, University of California, San Francisco).

in the hearts of chagasic mice compared with uninfected controls (Figure 4*B* and 4*C*). The expression of genes coding for

surface receptors, such as C3a receptor 1, Fc receptors for immunoglobulin E (high affinity) and G (low affinity), and Toll-like receptor 2, was also elevated in chagasic hearts (Table 3).

Fibrosis is characteristic of hearts in chronically chagasic mice (Figure 1*F*), and there was marked up-regulation of genes related to synthesis of extracellular matrix components (Table 3). In addition, the gene expression of lysyl oxidase, an enzyme that promotes the cross-linking of collagen fibers, was increased (Table 3). The tissue inhibitor of metalloproteinase 1 (TIMP-1), an inhibitor of collagen degradation, was also up-regulated in chronic chagasic hearts (Table 3). Quantitative real-time PCR analysis confirmed a significant overexpression in *Timp1* in hearts of chronically chagasic mice compared with normal controls (Figure 4*D*).
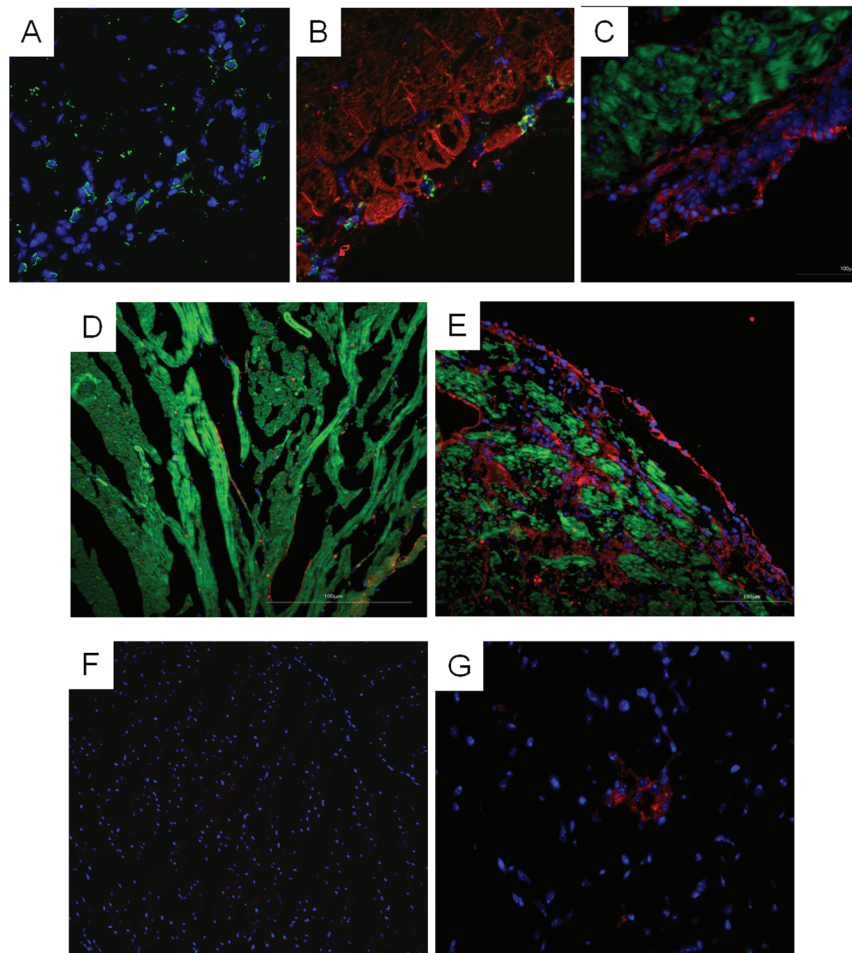

Figure 3. Analysis of heart sections from *Trypanosoma cruzi*–infected mice. Hearts from uninfected controls (*D* and *F*) and chronically chagasic mice (*A*–*C*, *E*, and *G*) were compared. *A*, Presence of CD4$^+$ cells (*green*) in infected myocardium. *B*, Section stained with anti-CD8 antibody (*green*) and phalloidin (*green*). *C*, Presence of CD11b$^+$ cells (*red*) in the inflammatory infiltrate and phalloidin staining (*green*) reveal proximity of macrophages to cardiac myocytes. *D* and *E*, Control (*D*) and infected (*E*) sections stained with an anti–intercellular adhesion molecule 1 antibody (*red*) and phalloidin (*green*), revealing up-regulation of this protein in the chagasic heart. *F* and *G*, Control (*F*) and infected (*G*) sections stained with an anti–major histocompatibility complex (MHC) II (Ia/Ie) antibody (*red*), showing the presence of MHC-II–expressing cells in the inflammatory infiltrate of chagasic hearts. All sections were stained with 4,6-diamidino-2-phenylindole for nuclear visualization (*blue*).

Table 3. Selected Up-regulated (>5-Fold) Genes

Gene name	Symbol	Fold regulation
Cytokine-related genes		
Chemokine (C-C motif) ligand 2	Ccl2	26.5
Chemokine (C-C motif) ligand 7	Ccl7/MCP3	16.2
Chemokine (C-C motif) ligand 8	Ccl8	50.6
Chemokine (C-C motif) receptor 5	Ccr5	12.1
Chemokine (C-X-C motif) ligand 12	Cxcl12/SDF1	5.0
IFN-γ–induced GTPase	Igtp	12.4
IFN-γ–inducible protein 30	Ifi30	11.9
IFN-γ–inducible protein 47	Ifi47	11.1
IFN regulatory factor 1	Irf1	7.7
IFN regulatory factor 5	Irf5	11.1
IL-10 receptor, α chain	IL-10ra	7.9
IL-18 binding protein	IL-18bp	6.6
IL-4 receptor, α chain precursor	IL-4Rα	9.2
LPS-induced TNF	Litaf	9.0
TNF-α–induced protein 2	Tnfaip2	6.2
TNF receptor superfamily, member 1b	Tnfrsf1b	9.4
TNF-α–induced protein 8–like	Tnf p8l	8.9
Immune response–related genes		
CD38 antigen	Cd38	7.0
CD52 antigen	Cd52/B7	21.6
CD68 antigen	Cd68	8.9
Complement component 4B	C4b	6.0
Complement factor B	Cfb	42.5
Fc receptor, IgE, high affinity I, gamma polypeptide	Fcer1g	17.6
Fc receptor, IgG, low affinity III	Fcgr3	9.1
Histocompatibility 2, class II antigen A, α	H2-Aa	38.5
Histocompatibility 2, class II, locus Mb1	H2-DMb1	12.7
Histocompatibility 2, Q region locus 7	H2-Q7	23.7
Histocompatibility 2, T region locus 10	H2-T10	5.0
Semaphorin 4A	SemaA4	8.9
T cell–specific GTPase	Tgtp	5.7
T cell, immune regulator 1, ATPase, H⁺ transporting, lysosomal V0 protein A3	Tcirg1, TIRC7	9.4
Toll-like receptor 2	Tlr2	5.4
Cell adhesion		
Galectin-3	Gal3	36.9
Integrin β3	Itgb3	6.0
Integrin β1–binding protein 3	Itgbp3	36.2
Intercellular adhesion molecule	Icam-1/Mala2	6.7
Enzymes		
Cathepsin C	Ctsc	12.5
Cathepsin H	Ctsh	8.1
Cathepsin S	Ctss	47.5
Cathepsin Z	Ctsz	8.3
Lysozyme 1	Lyz1	8.7
Lysoyme 2	Lys2	7.0
Lysyl oxidase	Lox	5.3
Phospholipase A2, group VII (platelet-activating factor acetylhydrolase, plasma)	Pla2g7	47.6
Proteasome (prosome, macropain) subunit, β type 10	Psmb10	6.56
Proteasome (prosome, macropain) subunit, β type 8 (large multifunctional peptidase 7)	Psmb8	8.1
Matrix metalloproteinase 14	Mmp14	10.8

Table 3. _(Continued.)_

Gene name	Symbol	Fold regulation
ECM-related genes		
α3 Type IX collagen	_Col9a3_	7.3
ECM protein 1	_Ecm1_	5.5
Microfibrillar-associated protein 5	_Mfap5_	8.0
Procollagen, type I, α2	_Col1a2_	6.0
TIMP-1	_Timp1_	49.6
TGF-β induced	_Tgfbi_	15.4

NOTE. ECM, extracellular matrix; IFN, interferon; Ig, immunoglobulin; IL, interleukin; LPS, lipopolysaccharide; TGF, transforming growth factor; TIMP, tissue inhibitor of metalloproteinase; TNF, tumor necrosis factor.

DISCUSSION

The factors responsible for the establishment of the symptomatic form of chronic Chagas heart disease are still not fully understood. However, it is likely that the damage sustained by the myocardium is derived from parasite as well as host factors [7]. Here we have identified, by microarray analysis, a number of genes up-regulated in hearts of chronically chagasic mice that probably play a role in modulating inflammation and fibrosis in this phase of infection and thus may represent targets for therapeutic intervention in this disease.

A significant proportion of cells in the inflammatory infiltrate found in hearts of chronically chagasic mice are macrophages, as shown here by the expression of CD11b and up-regulation of CD68 gene expression. These cells are found in close contact with myofibers and may directly contribute to their damage through the secretion of TNF-α. In addition, macrophages are in close contact with T lymphocytes in the inflammatory foci presenting antigens by MHC II molecules to CD4+ T lymphocytes, which secrete IFN-γ, increasing the cytotoxic potential of macrophages as well as of CD8+ T cells present in the inflammatory foci. Interestingly, we found expression of the Toll-like receptor 2 gene (_Tlr2_) up-regulated in hearts of chronically chagasic mice. _T. cruzi_ molecules, such as glycosylphosphatidylinositol anchors and glycoinositolphospholipids, activate macrophages to produce interleukin 12, TNF-α, and nitric oxide [16]. Thus, the residual parasitism found in the chronic infection probably contributes directly to the maintenance of TNF-α levels and indirectly to the maintenance of IFN-γ levels (through interleukin 12 production) in the hearts of chronically chagasic mice.

Although a growing body of evidence indicates that TNF-α contributes to the pathogenesis of heart failure [17], other reports have suggested beneficial effects of this cytokine in the heart [18]. Cardiac myocytes express both TNF-α receptors, type 1 (TNFR1) and type 2 (TNFR2) [19], which mediate its functions. TNFR1 seems to mediate the majority of the deleterious effects of TNF-α, such as TNF-α–induced cell death [20]. In contrast, activation of TNFR2 appears to exert protective effects against cardiac myocyte damage and apoptosis [21–23]. The strong up-regulation of the TNFR2 gene (_Tnfrsf1b_) in the hearts of chronically chagasic mice indicates that this receptor may contribute to the low number of apoptotic cardiac myocytes found during this phase of infection [24].

PLA2G7, another molecule secreted by monocytes and macrophages and found to be up-regulated in our study, degrades PAF, a lipid mediator that activates various cell types and promotes inflammation. Mice lacking PAF receptor (PAFR) have increased inflammation and parasitism in their hearts during acute infection [25]. This may be due to decreased parasite uptake and macrophage activation in the absence of PAFR activation, because PAF has been shown to mediate nitric oxide production and resistance to _T. cruzi_ infection in mice [26]. In our model of chronic chagasic myocarditis, the role of PAF degradation by PLA2G7 is unknown, but the reduction in PAF accumulation may be related to the progressive damage of the myocardium, because PAF was shown to have a cardioprotective effect in isolated hearts [27].

A number of molecules involved in the recruitment of inflammatory cells to the heart of chagasic mice, including adhesion molecules and chemoattractant factors, were found to be up-regulated in our study. ICAM-1 expression in heart and endothelial cells was also increased in chagasic hearts, as described elsewhere [28, 29]. TNF-α increases the adhesiveness of endothelium for leukocytes and induces ICAM-1 expression [30]. Thus, the proinflammatory cytokines produced at the inflamed heart may be promoting the maintenance of inflammation by increasing the expression of ICAM-1. In agreement with the present study, overexpression of galectin-3 has been reported in _T. cruzi_–infected mice [31]. Galectin-3 binds to extracellular matrix components and was shown to participate in the adhesion of the parasite to coronary artery smooth muscle cells [32].

In the present study we found that chemokine genes encoding for CCL2, CCL8, and CCL7 (monocyte chemoattractant protein [MCP] 1, 2, and 3, respectively) are up-regulated in hearts of chronically chagasic mice. A number of studies have shown
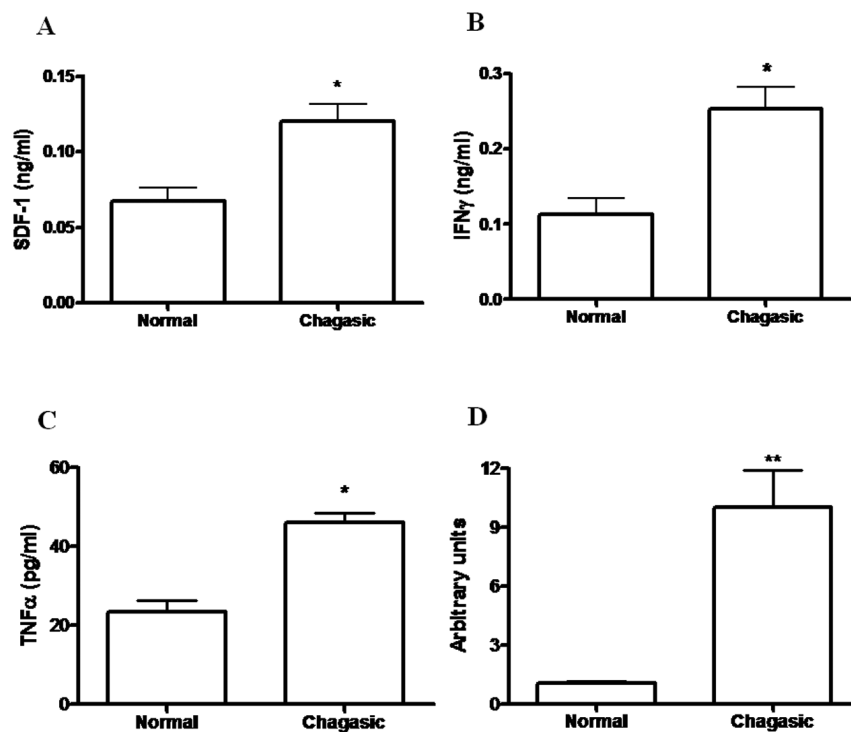
Figure 4. Increased production of stromal cell–derived factor 1 (SDF-1), interferon (IFN) γ, and tumor necrosis factor (TNF) α and transcript levels of *Timp1* in hearts of chronically chagasic mice. *A–C*, Levels of SDF-1 (*A*), IFN-γ (*B*), and TNF-α (*C*) identified in heart homogenates of normal mice ($n = 4$) and chagasic mice ($n = 9$; 8 months after infection with *Trypanosoma cruzi*), by enzyme-linked immunosorbent assay. *$P < .05$ and **$P < .01$. *D*, *Timp1* analyzed by quantitative real-time reverse-transcription polymerase chain reaction, using complementary DNA samples prepared from messenger RNA extracted from the hearts of normal ($n = 5$) or chronically chagasic ($n = 5$) mice. Data represent means $\pm$ standard errors of the mean for values obtained from individual mice.

that *T. cruzi* infection stimulates the production of chemokines by macrophages as well as by cardiomyocytes [33–35]. These chemokines are known to recruit monocytes and T lymphocytes. Other studies have demonstrated an association between the expression of MCP-1 and MCP-2 in the heart and both myocarditis and heart dysfunction [36, 37], suggesting a role of these cytokines in the maintenance of chagasic myocarditis.

CCR5 is a receptor for several chemokines of the CC family, including CCL3, CCL4, and CCL5, known to be up-regulated by infection with the Colombian strain of *T. cruzi* [38], and also for CCL8. Hearts of CCR5-deficient mice infected with *T. cruzi* have reduced migration of T cells. Because this receptor is predominantly expressed on the surface of Th1 cells [39], and a type 1 response with production of IFN-γ is associated with severity of CCM, CCR5 may play an important role in the pathogenesis of chronic chagasic myocarditis, as described in a model of autoimmune myocarditis [40]. In fact, treatment of chagasic mice with a selective CCR1 and CCR5 antagonist (Met-RANTES) decreased heart inflammation and fibrosis [41]. A positive correlation between severity of cardiomyopathy and the presence of CCR5$^+$ IFN-γ^+ T cells was found in patients with chronic Chagas disease [14].

We found that CXCL12 (SDF-1) expression is increased in hearts of chronically chagasic mice. SDF-1 is a potent chemoattractant factor for lymphocytes [42], and therefore its expression may be relevant for the maintenance of immune-mediated heart destruction during the chronic phase of infection. Conversely, because this chemokine is also a stem cell recruitment factor, its increased expression may contribute to tissue regeneration of the damaged myocardium, as reported elsewhere in a model of myocardial ischemia [43]. In addition, MCP-3 (CCL7) was recently shown to be a mesenchymal stem cell homing factor for the myocardium [44]. Thus, the increased expression of these chemokines indicates that migration of stem cells can be promoted in chronic chagasic myocarditis by the presence of stem cell chemoattractant factors such as SDF-1 and MCP-3. In fact, we have shown that intravenously injected bone marrow cells migrate to the hearts of chronically chagasic mice [45].

The myocardial interstitial collagen matrix surrounds and supports cardiac myocytes and the coronary microcirculation, and its integrity is critical for the proper function of the heart. Thus, alterations in the collagen matrix will disrupt myocardial mechanical properties and ventricular function [46]. In Chagas dis-

ease, as a consequence of the sustained inflammatory process found in the myocardium during the chronic phase of infection, fibrosis is evident and contributes to cardiac remodeling. We also observed alterations in genes related to extracellular matrix deposition, such as extracellular matrix components and *Timp1*. Plasma concentrations of TIMP-1 are significantly elevated in patients with terminal heart failure compared with healthy controls [47], suggesting that this metalloproteinase inhibitor may also play a role in the evolution of heart failure in chronic Chagas disease. In addition, lysyl oxidase was increased in chagasic hearts. This enzyme promotes the cross-linking of collagen fibers, irreversibly altering the structure and function of the extracellular matrix proteins, causing dysfunction of the cardiomyocytes and, consequently, of the heart [46]; it therefore probably plays an important role in the evolution of fibrosis in chronic chagasic hearts.

To understand the delicate balance of multiple factors involved in the pathogenesis of Chagas disease is a complex task. Microarray approaches have been used before in mouse models of *T. cruzi* infection (C3H/HeN mice infected with *T. cruzi* Sylvio X10/4 strain [47] and C57Bl/6.129sv mice infected with *T. cruzi* Brazil strain [48, 49], as well as in hearts of chronically chagasic patients [50]. Using the model of infection with Colombian *T. cruzi* strain, we have identified new potentially important genes that may serve as a basis for therapeutic interventions in chronic Chagas heart disease.

Acknowledgments

References

1. World Health Organization. Chagas' disease: important advances in elimination of transmission in four countries in Latin America. Geneva, Switzerland: WHO Feature **1995**; 183:1–3.
2. Dias JCP, Coura JR. Epidemiologia. In: Dias JCP, Coura JR, eds. Clínica e terapêutica da doença de Chagas: uma abordagem prática para o clínico geral. 2nd ed. Brazil: Fundação Oswaldo Cruz, **1997**:36–66.
3. Rosenbaum MB. Chagasic myocardiopathy. Prog Cardiovasc Dis **1964**; 7:199–225.
4. Chiale PA, Rosenbaum MB. Clinical and pharmacological characterization and treatment of potentially malignant arrythmias of chronic chagasic cardiomiopathy. In: Williams EMV, Campbell TJ, eds. Handbook of experimental pharmacology. Ed 5. Springer-Verlag, **1989**: 601–620.
5. Tanowitz HB, Kirchhoff LV, Simon D, Morris SA, Weiss LM, Wittner M. Chagas' disease. Clin Microbiol Rev **1992**; 5:400–419.
6. Petkova SB, Huang H, Factor SM, et al. The role of endothelin in the pathogenesis of Chagas' disease. Int J Parasitol **2001**; 31:499–511.
7. Soares MB, Pontes-De-Carvalho L, Ribeiro-dos-Santos R. The pathogenesis of Chagas' disease: when autoimmune and parasite-specific immune responses meet. An Acad Bras Cienc **2001**; 73:547–559.
8. Garcia S, Ramos CO, Senra JF, et al. Treatment with benznidazole during the chronic phase of experimental Chagas' disease decreases cardiac alterations. Antimicrob Agents Chemother **2005**; 49:1521–1528.
9. Federici EE, Abelmann WN, Neva FA. Chronic and progressive myocarditis in C3H mice infected with *Trypanosoma cruzi*. Am J Trop Med Hyg **1964**; 13:272–280.
10. Iacobas DA, Fan C, Iacobas S, Spray DC, Haddad GG. Transcriptomic changes in developing kidney exposed to chronic hypoxia. Biochem Biophys Res Comm **2006**; 349(1):329–338.
11. Iacobas DA, Iacobas S, Li WE, Zoidl G, Dermietzel R, Spray DC. Genes controlling multiple functional pathways are transcriptionally regulated in connexin43 null mouse heart. Physiol Genomics **2005**; 20:211–223.
12. Dahlquist KD, Salomonis N, Vranizan K, Lawlor SC, Conklin BR. GenMAPP, a new tool for viewing and analyzing microarray data on biological pathways. Nat Genet **2002**; 31:19–20.
13. Cunha-Neto E, Rizzo LV, Albuquerque F, et al. Cytokine production profile of heart-infiltrating T cells in Chagas' disease cardiomyopathy. Braz J Med Biol Res **1998**; 31:133–137.
14. Gomes JA, Bahia-Oliveira LM, Rocha MO, et al. Type 1 chemokine receptor expression in Chagas' disease correlates with morbidity in cardiac patients. Infect Immun **2005**; 73:7960–7966.
15. Campos MA, Almeida IC, Takeuchi O, et al. Activation of Toll-like receptor-2 by glycosylphosphatidylinositol anchors from a protozoan parasite. J Immunol **2001**; 167:416–423.
16. Anker SD, Coats AJ. How to RECOVER from RENAISSANCE? The significance of the results of RECOVER, RENAISSANCE, RENEWAL and ATTACH. Int J Cardiol **2002**; 86:123–130.
17. Kurrelmeyer KM, Michael LH, Baumgarten G, et al. Endogenous tumor necrosis factor protects the adult cardiac myocyte against ischemic-induced apoptosis in a murine model of acute myocardial infarction. Proc Natl Acad Sci U S A **2000**; 97:5456–5461.
18. Torre-Amione G, Kapadia S, Lee J, Bies RD, Lebovitz R, Mann, DL. Expression and functional significance of tumor necrosis factor receptors in human myocardium. Circulation **1995**; 92:1487–1493.
19. Shen HM, Pervaiz S. TNF receptor superfamily-induced cell death: redox-dependent execution. FASEB J **2006**; 20:1589–1598.
20. Higuchi Y, McTiernan CF, Frye CB, McGowan BS, Chan TO, Feldman AM. Tumor necrosis factor receptors 1 and 2 differentially regulate survival, cardiac dysfunction, and remodeling in transgenic mice with tumor necrosis factor-alpha-induced cardiomyopathy. Circulation **2004**; 109:1892–1897.
21. Ramani R, Mathier M, Wang P, et al. Inhibition of tumor necrosis factor receptor-1-mediated pathways has beneficial effects in a murine model of postischemic remodeling. Am J Physiol Heart Circ Physiol **2004**; 287:H1369–377.
22. Defer N, Azroyan A, Pecker F, Pavoine C. TNFR1 and TNFR2 signaling interplay in cardiac myocytes. J Biol Chem **2007**; 282:35564–35573.
23. Rossi MA, Souza AC. Is apoptosis a mechanism of cell death of cardiomyocytes in chronic chagasic myocarditis? Int J Cardiol **1999**; 68: 325–331.
24. da Silva RP, Gordon S. Phagocytosis stimulates alternative glycosylation of macrosialin (mouse CD68), a macrophage-specific endosomal protein. Biochem J **1999**; 338:687–694.
25. Aliberti JC, Machado FS, Gazzinelli RT, Teixeira MM, Silva JS. Platelet-activating factor induces nitric oxide synthesis in *Trypanosoma cruzi*-infected macrophages and mediates resistance to parasite infection in mice. Infect Immun **1999**; 67:2810–2814.
26. Penna C, Alloatti G, Cappello S, et al. Platelet-activating factor induces cardioprotection in isolated rat heart akin to ischemic preconditioning: role of phosphoinositide 3-kinase and protein kinase C activation. Am J Physiol Heart Circ Physiol **2005**; 288:H2512–H2520.
27. Laucella S, Salcedo R, Castaños-Velez E, et al. Increased expression and secretion of ICAM-1 during experimental infection with *Trypanosoma cruzi*. Parasite Immunol **1996**; 18:227–239.
28. Huang H, Calderon TM, Berman JW, Braunstein VL, Weiss LM, Wittner M, Tanowitz HB. Infection of endothelial cells with *Trypanosoma cruzi* activates NF-kappaB and induces vascular adhesion molecule expression. Infect Immun **1999**; 67:5434–5440.
29. Ledebur HC, Parks TP. Transcriptional regulation of the intercellular

adhesion molecule-1 gene by inflammatory cytokines in human endothelial cells. J Biol Chem **1995**; 270:933–943.

30. Vray B, Camby I, Vercruysse V, et al. Up-regulation of galectin-3 and its ligands by *Trypanosoma cruzi* infection with modulation of adhesion and migration of murine dendritic cells. Glycobiology **2004**; 14:647–657.

31. Kleshchenko YY, Moody TN, Furtak VA, Ochieng J, Lima MF, Villalta F. Human galectin-3 promotes *Trypanosoma cruzi* adhesion to human coronary artery smooth muscle cells. Infect Immun **2004**; 72:6717–6721.

32. Villalta F, Zhang Y, Bibb KE, Kappes JC, Lima MF. The cysteine-cysteine family of chemokines RANTES, MIP-1alpha, and MIP-1beta induce trypanocidal activity in human macrophages via nitric oxide. Infect Immun **1998**; 66:4690–4695.

33. Aliberti JC, Machado FS, Souto JT, et al. beta-Chemokines enhance parasite uptake and promote nitric oxide-dependent microbiostatic activity in murine inflammatory macrophages infected with *Trypanosoma cruzi*. Infect Immun **1999**; 67:4819–4826.

34. Machado FS, Martins GA, Aliberti JC, Mestriner FL, Cunha FQ, Silva JS. *Trypanosoma cruzi*-infected cardiomyocytes produce chemokines and cytokines that trigger potent nitric oxide-dependent trypanocidal activity. Circulation **2000**; 102:3003–3008.

35. Kolattukudy PE, Quach T, Bergese S, et al. Myocarditis induced by targeted expression of the MCP-1 gene in murine cardiac muscle. Am J Pathol **1998**; 152:101–111.

36. Shen Y, Xu W, Chu YW, Wang Y, Liu QS, Xiong SD. Coxsackievirus group B type 3 infection upregulates expression of monocyte chemoattractant protein 1 in cardiac myocytes, which leads to enhanced migration of mononuclear cells in viral myocarditis. J Virol **2004**; 78:12548–12556.

37. Talvani A, Ribeiro CS, Aliberti JC, et al. Kinetics of cytokine gene expression in experimental chagasic cardiomyopathy: tissue parasitism and endogenous IFN-gamma as important determinants of chemokine mRNA expression during infection with *Trypanosoma cruzi*. Microbes Infect **2000**; 2:851–866.

38. Turner JE, Steinmetz OM, Stahl RA, Panzer U. Targeting of Th1-associated chemokine receptors CXCR3 and CCR5 as therapeutic strategy for inflammatory diseases. Mini Rev Med Chem **2007**; 7:1089–1096.

39. Gong X, Feng H, Zhang S, Yu Y, Li J, Wang J, Guo B. Increased expression of CCR5 in experimental autoimmune myocarditis and reduced severity induced by anti-CCR5 monoclonal antibody. J Mol Cell Cardiol **2007**; 42:781–791.

40. Marino AP, da Silva A, dos Santos P, et al. Regulated on activation, normal T cell expressed and secreted (RANTES) antagonist (Met-RANTES) controls the early phase of *Trypanosoma cruzi*-elicited myocarditis. Circulation **2004**; 110:1443–1449.

41. Bleul CC, Fuhlbrigge RC, Casasnovas JM, Aiuti A, Springer TA. A highly efficacious lymphocyte chemoattractant, stromal cell-derived factor 1 (SDF-1). J Exp Med **1996**; 184:1101–1109.

42. Askari AT, Unzek S, Popovic ZB, et al. Effect of stromal-cell-derived factor 1 on stem-cell homing and tissue regeneration in ischaemic cardiomyopathy. Lancet **2003**; 362:697–703.

43. Schenk S, Mal N, Finan A, et al. Monocyte chemotactic protein-3 is a myocardial mesenchymal stem cell homing factor. Stem Cells **2007**; 25:245–251.

44. Soares MB, Lima RS, Rocha LL, et al. Transplanted bone marrow cells repair heart tissue and reduce myocarditis in chronic chagasic mice. Am J Pathol **2004**; 164:441–447.

45. Souza RR. Aging of myocardial collagen. Biogerontology **2002**; 3:325–335.

46. Milting H, Ellinghaus P, Seewald M et al. Plasma biomarkers of myocardial fibrosis and remodeling in terminal heart failure patients supported by mechanical circulatory support devices. J Heart Lung Transplant **2008**; 27:589–596.

47. Garg N, Popov VL, Papaconstantinou J. Profiling gene transcription reveals a deficiency of mitochondrial oxidative phosphorylation in *Trypanosoma cruzi*-infected murine hearts: implications in chagasic myocarditis development. Biochim Biophys Acta **2003**; 1638:106–120.

48. Mukherjee S, Belbin TJ, Spray DC, et al. Microarray analysis of changes in gene expression in a murine model of chronic chagasic cardiomyopathy. Parasitol Res **2003**; 91:187–196.

49. Mukherjee S, Nagajyothi F, Mukhopadhyay A, et al. Alterations in myocardial gene expression associated with experimental *Trypanosoma cruzi* infection. Genomics **2008**; 91:423–432.

50. Cunha-Neto E, Dzau VJ, Allen PD, et al. Cardiac gene expression profiling provides evidence for cytokinopathy as a molecular mechanism in Chagas' disease cardiomyopathy. Am J Pathol **2005**; 167:305–313.